

Effect of welding parameters on microstructure, mechanical properties and hot cracking phenomenon in Udimet 520 superalloy

Fardin Nematzadeh^a, Mohammad Reza Akbarpour^{a,*}, Soroush Parvizi^b, Amir Hosein Kokabi^b, Seyed Khatiboleslam Sadrnezhaad^b

^a Materials and Energy Research Center, Karaj, Iran

^b Department of Materials Science and Engineering, Sharif University of Technology, Tehran, Iran

ARTICLE INFO

Article history:

Received 25 June 2010

Accepted 14 October 2011

Available online 4 November 2011

Keywords:

A. Non-ferrous metals and alloys

D. Welding

E. Mechanical

ABSTRACT

In the present research, different weld layers were deposited on a 1.2714 steel die by gas tungsten arc (GTA) welding with the weld wire of Udimet 520, and effects of welding parameters on microstructure and mechanical properties of Udimet 520 superalloy were investigated. The results showed Udimet 520 weld with cellular–dendritic and rarely dendritic structure including γ matrix rich of Cr, Mo and W, low percentage associated with order morphology and relative uniform distribution of MC type carbides. Udimet 520 alloy showed high resistance against hot cracking during welding and hot cracking occurred only at high input heat values. Also, cracking during welding occurred at the places that the concentration of Al and Ti is high. Investigation of the effect of welding parameters on the hardness of GTA welded Udimet 520 showed that with increasing welding speed and decreasing input heat, the hardness of the weld improved. Increase in hardness of GTA welded Udimet 520 due to increasing welding rate and decreasing heat input is attributed to the fineness of columnar structure and solid solution strengthening.

© 2011 Elsevier Ltd. All rights reserved.

1. Introduction

Udimet 520 superalloy is a precipitation-hardenable nickel base superalloy with an exceptional combination of high-temperature mechanical properties, corrosion resistance and forgeability characteristics. This alloy is developed for use in the 1400–1700 °F (760–927 °C) temperature range, and has excellent structural stability and unusually good fabricability. The primary application for this alloy is balding for aircraft and land-based gas turbines. Some applications for Udimet 520 superalloy require the alloy to be welded.

The stability and creep resistance of superalloys depend on the precipitate morphology and volume fraction of precipitates, which strengthen the γ -phase matrix [1]. The investigation of solidification of these alloys needs determination of equilibrium distribution coefficient from phase diagram and knowledge of accurate position of closed lines of ternary phases, which are specified for some multi alloy systems [2]. The main differences between solidification in casting and welding are high solidification rate and high thermal gradient at solidification front in welding. As a result of none – equilibrium cooling of welds, amount and morphology of phases especially in Ni-based super alloys change severely.

The solidification of weld has the following stages [2]:

- First stage of the solidification is performed epitaxially on molten grains of base metal.
- At start, crystals grow slowly and faceted structure forms. Then the formation of fine cellular structure occurs.
- Crystalline growth is cellular–dendritic at intermediate stage and leads to the formation of coarse columnar growth in $\langle 100 \rangle$ direction at cubic systems.
- Final stage of solidification is associated with quick growth of grains and local concentration of particles. Therefore, final dendritic structure forms proportional to weld conditions.

Research of Lucas [3] on these alloys has shown that solidification cracking happens during welding. During the solidification of the weld pool, columnar grains grow from boundary of base metal and melt at central region of metal. Most of alloying elements and inclusions are rejected to the solidification front and concentrate in molten region. This causes compositional undercooling. The molten region remains liquid until the columnar grains reach together and the solidification complete. This fused layer decreases the adherence between contacting area of grains, and increases malleability of weld metal. Finally, shrinkage stresses induced during cooling process produce intergranular cracks. Other forms of solidification cracks have been studied by Ojo et al. [4]. According to their research, the elements as S, Pb, and some low

* Corresponding author. Tel.: +98 9125790993; fax: +98 2188773352.

E-mail address: M-akbarpour@merc.ac.ir (M.R. Akbarpour).

melting point elements (as Bi) accelerate corrosion cracking. These contaminants form intergranular film and lead the weld to be intensively brittle at high temperatures.

One of the applications requiring welding of this alloy is radial forging dies. In a recent study [5], welding of this alloy has been used for hardening of radial forging die surface. The weld structure of Udimet 520 has been compared with the structure of specimens under service and concluded that the weld structure of Udimet 520 on the surface of die during working remains without any considerable change. Just the dendrites deform and break. Formed MC carbides during solidification remain without any considerable change during service, but they maybe grow by diffusion.

Since the weld microstructure and mechanical properties strongly depend on the welding condition, this research is undertaken to investigate the effect of heat input and welding rate on mechanical properties as well as hot cracking mechanism during solidification of Udimet 520 weld by gas tungsten arc welding (GTAW).

2. Materials and research procedure

2.1. Specimen preparation

Cubic specimens ($24 \times 25 \times 4 \text{ cm}^3$) of 1.2714 steel were pre-heated for 2 h to reach weld temperature range of (320–400 °C) by especial gas flame. Temperature was controlled by thermometer. The cubic specimens were divided into two areas of 40 cm^2 with length of 2 cm to balance stress during welding at different regions. The welding process was carried out in two stages. At the first stage, an intermediate and flexible layer with the thickness of 20 mm was formed by Shielded metal arc welding (SMAW), and then a high resistant layer against themomechanical fatigue with the thickness of 10 mm was deposited by gas tungsten arc welding (GTAW). After depositing the first layer, pneumatic brush was used to clean the welded area. Besides, pneumatic hammer was utilized to increase the formability of the weld and to induce compressive residual stresses during welding of the second layer. Welding conditions and used materials are given in Tables 1–3.

Because of very low machinability of the weld of Udimet 520, magnetic grinding was used to prepare specimens surface for metallography, X-ray diffraction (XRD), hardness test, chemical analysis and temperature distribution.

2.2. Metallography

In order to study the microstructure of Udimet 520 super alloy weld, particularly formed carbides, specimens after hot mounting were grinded by SiC grit papers, and then were polished by diamond paste at different sizes from 0.025 to $6 \mu\text{m}$. After that, prepared specimens were cleaned by acetone prior etching with (10 g CuSO_4 , 50 cc HCl, and 50 cc H_2O) solution [5].

2.3. Microstructure determination

Optical microscope and scanning electron microscope (SEM) equipped with EDS (Philips XL30) were used to study the

microstructures and possible hot crack formed during welding and to analyze the sides of formed hot crack during solidification. In order to detect phases during welding, the polished specimens were tested using a Philips PW 1410 X-ray spectrometer operated at 30 kV and 20 mA with CuK α radiation.

2.4. Temperature distribution

Pyrometer, thermometer and thermocouple were used to determine temperature distribution during welding.

2.5. Chemical analysis

Distribution of elements in the weld layers of Udimet 520 superalloy was determined by quantometer.

2.6. Hardness measurement

Rockwell hardness equipments were utilized to measure the hardness of the weld of Udimet 520 superalloy.

3. Results and discussion

3.1. The Udimet 520 weld microstructure

Fig. 1 shows the microstructure of the first layer welded by SMAW. It comprises the γ matrix with the islands of metal carbides. Also, the microstructure of wrought Udimet 520 consisting of γ matrix with spherical and very fine carbides (MC) is shown in Fig. 2. After deposition of first layer on the base metal, second layer (wrought Udimet 520 wire with microstructure shown in Fig. 2) was deposited on the first layer by GTAW. The microstructure of the second layer weld was cellular–dendritic and rarely dendritic structures as shown in Fig. 3. Because of the cooling condition and growth profile of progressive solid phase in a weld, the structure is cellular–dendritic structure [1]. Usually in a properly controlled thermal gradient condition, derivative arms melt and equiaxed grains forms. The cooling condition at present study was such that no remelting occurred. Therefore, the equiaxed grains were not seen.

Heat conductivity of Ni-base superalloys is low, therefore a moderate cooling occurs. Hence, the weld microstructure is not columnar. On the other hand, the heat conductivity of steel is relatively higher than that of Ni-base superalloy [6,7]; hence this causes little tendency toward dimensional structure. The mentioned facts confirm the formation of cellular–dendritic microstructure.

In the recent paper [5], it was shown that interdendritic spaces of weld is mainly homogenous structure of γ matrix rich of segregated elements accompanied by low percentage of MC carbides. The formed phases during solidification in the microstructure strengthened the matrix. The microstructure includes the homogenous structure of γ phase matrix rich of Cr, Mo, W, as solid solution strengthening elements, and very fine dark MC carbides [8].

Figs. 4 and 5 show the Time–Temperature Transformation (TTT) diagrams of Udimet 520 superalloy [8]. According to the TTT

Table 1
Chemical composition of base metal and weld materials.

Materials	Elements (wt.%)										
	C	Ni	Mo	Cr	W	Ti	Co	Al	Fe	Mn	Si
1.2714 Steel (base metal)	0.6	1.51	0.52	1.10	0.06	0.01	0.01	0.01	94.9	0.71	0.29
Fox Saca (filler metal)	0.01	56	17	17	5	–	–	–	5	–	–
Udimet 520	0.06	55.50	5.01	19.1	1.03	3.04	12.07	2.00	0.7	0.35	0.35

Table 2
GTA welding parameters of Udimet 520.

Current (A)	Voltage (V)	Input heat ($\times 10^3$ J/m)	Welding rate ($\times 10^{-3}$ m/s)	Interpass temperature ($^{\circ}\text{C}$)	Preheat temperature ($^{\circ}\text{C}$)	Argon flow (Lit/min)
430	36	4000	2.5	380	350	14

Table 3
SMAW welding parameters of filler metal (first layer).

Current (A)	Voltage (V)	Input heat ($\times 10^3$ J/m)	Welding rate ($\times 10^{-3}$ m/s)	Interpass temperature ($^{\circ}\text{C}$)	Preheat temperature ($^{\circ}\text{C}$)	Argon flow (Lit/min)
240	36	1300	2	350	320–400	10–14

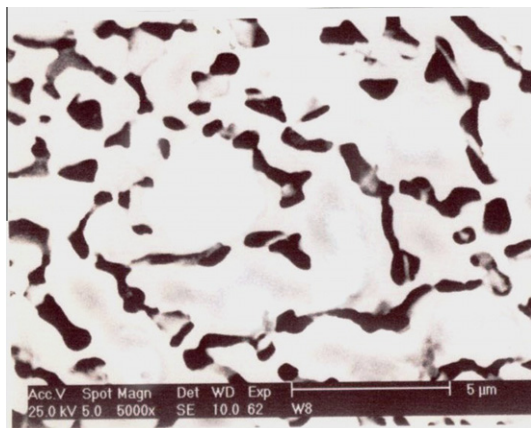


Fig. 1. SEM micrograph of first layer consisting γ matrix with the islands of metal carbides.

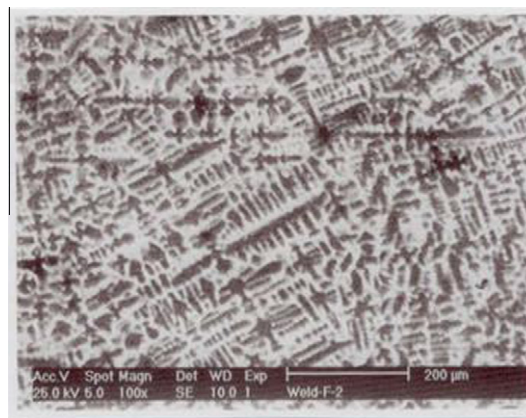


Fig. 3. SEM micrograph showing the microscopic image of dendritic structure of Udimet 520 weld.

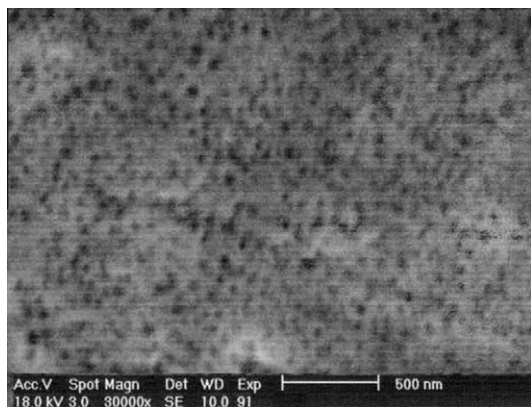


Fig. 2. SEM micrograph of wrought Udimet 520 consisting γ matrix with fine spherical MC carbides.

diagrams and cooling cycle of Udimet 520 weld (Fig. 6), it is seen that cooling curve does not cut the nose of TTT diagram. Accordingly, the weld structure should have clearly γ phase matrix and limited amount of MC carbides formed during the solidification. The formation of primary γ and other phases during welding is impossible at this cooling condition. On the other hand, γ phase can form during heat treatment. According to the alloy's TTT diagram, γ phase precipitation needs heat treatment at temperature of 1250°C for a time larger than 10 s [8]. Whereas in this research no heat treatment was done, rapid and none-equilibrium cooling of the weld retards the diffusion of W and Mo and makes the formation of γ phase impossible [3].

Fig. 7 shows the XRD pattern of Udimet 520 weld. XRD studies reveal only γ phase peaks and MC carbides are not distinguishable because of low volume percentage.

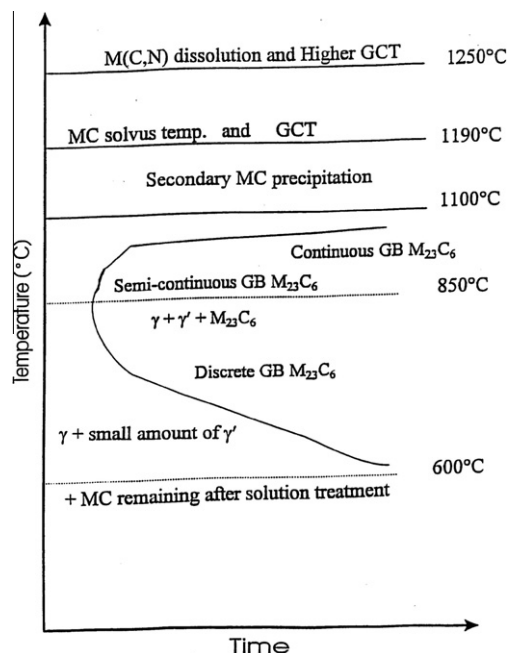


Fig. 4. Schematic TTT diagram of Udimet 520 [9].

Effect of carbides (morphology and distribution) on mechanical properties of this superalloy has been studied by some researchers [9]. Their study shows that heterogeneous, disorder morphology and high level of carbides lower the mechanical properties. Whatever the order degree of morphology increases (Spherical shape) and optimum level of carbides and their fine distribution is establish, mechanical properties improve [9].

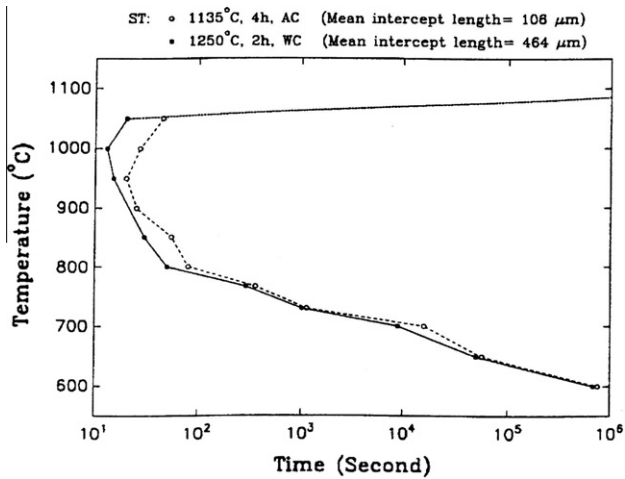


Fig. 5. Schematic TTT diagram of Udimet 520 for $M_{23}C_6$ phase precipitation [9].

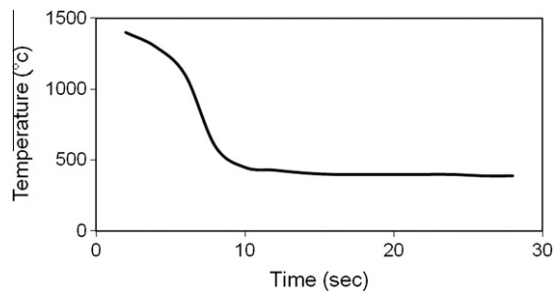


Fig. 6. Cooling cycle of Udimet 520 weld.

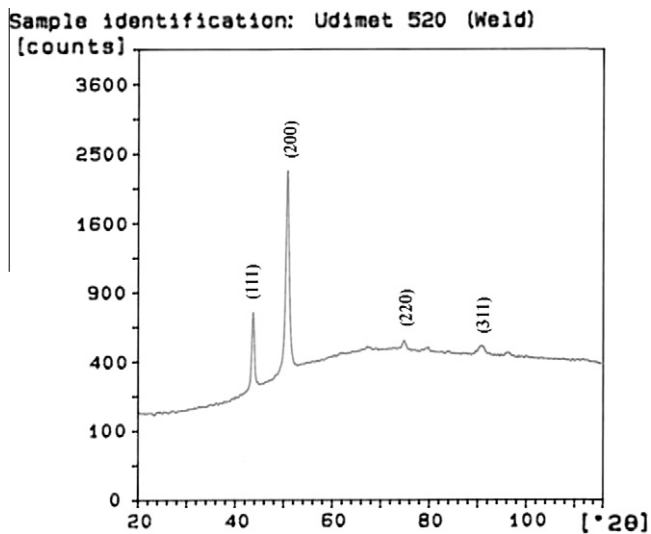


Fig. 7. X-ray diffraction pattern of Udimet 520 weld.

Table 4 shows the average distribution of elements in the weld of Udimet 520 superalloy that is not different from composition of wrought material. Also distribution of different elements in the weld with distance from base metal to end of the second layer of weld is shown in Table 5. It is seen that the weld structure of Udimet 520 has optimum properties of γ matrix rich of Cr, Mo and W as solid solution strengthening agents, low percentage associated with order morphology and relative uniform distribution of MC carbides and substantial stability at high temperatures. Because

Table 4

Average distribution of elements in the weld of Udimet 520.

Elements	Weld of Udimet 520 (wt.%)
Ni	56.00
W	2.01
Mo	8.89
Cr	17.54
Co	9.41
Al	1.82
Ti	2.41
C	0.04

of this optimum condition, this alloy has the good mechanical properties. Udimet 520 wrought structure does not have these properties [9–11].

Crack formation during welding of Udimet 520

Hot cracking during welding has been studied experimentally and different manifestations of hot cracking phenomena during welding are:

- solidification cracking,
- liquation cracking in the heat affected zone (HAZ), and
- a combination of the above two.

The tendency of an alloy to form solidification cracks is directly related with the difference between the solidus and liquidus temperatures of the alloy. Thus, alloys having extended solidification temperature ranges are more susceptible to fusion-zone solidification cracking than alloys which solidify over a narrow temperature range.

Udimet 520 contain substantial amount of Al and Ti (<6 wt.%), is generally considered very resistant to HAZ cracking during welding. Elements such as B, Cr and Zr with small amount have major effect on weldability of this alloy [3,4]. Carbon dissolves in HAZ at high temperatures and deposits as graphite in grain boundaries during cooling. This decreases ductility of HAZ [12]. Also, since this alloy does not have any S and P, it is not sensitive to solidification hot crack in HAZ [13].

According to Table 4, carbon content in the weld is always lower than that of Udimet 520, because carbon is rejected at the solidification front and concentrated at the central region of the melt during the weld solidification. This results a decrease in solidification temperature. The presence of the eutectic during the last stages of solidification, in combination with the thermal stresses which produce during welding and large solidification range, promotes solidification cracks in this alloy. Solidification cracking can occur at the last stages of solidification when the dendrite arms are coalesced and feeding of melt is difficult. If strain produces at these situations due to solidification shrinkage or thermal contraction, hot tears can form at grain boundaries. Schematic formation mechanism of cracks due to shrinkage stresses is shown in Fig. 8.

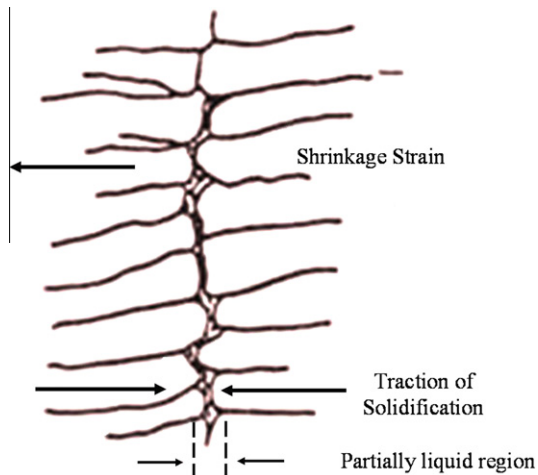
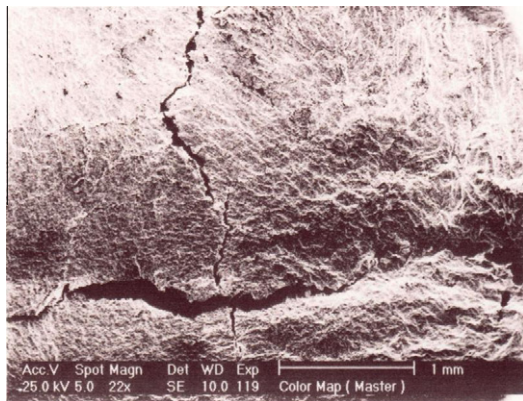
In Udimet 520 during welding, hot cracking is formed during welding at higher heat inputs. When the heat input increased to the high values (higher than 7000 J/mm), hot cracking occurred in this alloy. Fig. 9 shows the hot solidification crack during welding of Udimet 520 by GTAW. Hot cracks in dendritic solidification form due to some alloying elements concentration such as Al, Ti, a rise in input heat and an increase in percentage of Al at the end of the weld pass.

Weldability of precipitation-hardened alloys strongly depends on quantity and morphology of the γ' intermetallic phase ($Ni_3Al(-Ti)$). γ' phase content is related with the concentration of Ti and Al over a critical value which this phases precipitates. According to Lachowicz et al. [14], the total Al and Ti content should not exceed

Table 5

Average weight percentage of different elements from base metal to the end of weld second layer.

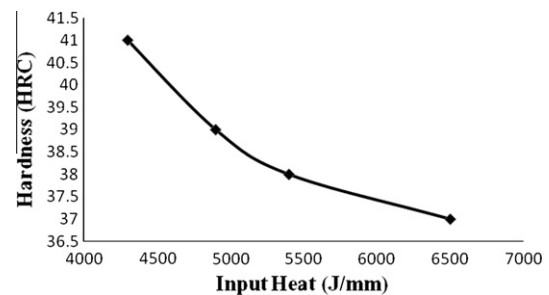
Distance from base metal to the end of second layer of weld (mm)	C	Si	Mn	Cr	Mo	W	Ti	Co	Al	Fe	Ni
30	0.037	0.17	0.08	18.11	7.60	1.52	2.67	10.95	2.00	0.95	55.98
25	0.037	0.1740	0.13	17.54	8.50	1.83	2.56	9.927	1.932	1.24	56.08
20	0.0361	0.296	0.282	16.90	10.59	2.639	1.942	7.577	1.503	2.01	56.38
15	0.198	0.313	0.689	11.57	13.43	3.879	0.019	0.09	0.0053	22.03	47.69
10	0.198	0.313	0.756	12.37	7.063	2.885	0.012	0.054	0.019	41.02	34.97
5	0.384	0.37	0.575	5.04	6.507	1.657	0.0097	0.078	0.0057	60.03	25.22

**Fig. 8.** Schematic mechanism of hot solidification crack formation during welding.**Fig. 9.** SEM micrograph showing the formation of hot solidification crack during welding of Udimet 520 (x22).**Table 6**

Analysis of sides of formed hot solidification crack (Fig. 9).

Element	Al K	MoL	TiK	CrK	FeK	CoK	NiK	Total
Wt.%	33.47	4.17	8.56	8.56	18.58	5.32	21.35	100

4%. Analysis of formed hot crack sides during welding of this alloy is represented in Table 6. According to Table 5, during the welding of this alloy at high heat input values, the supersaturating of Ti and Al at the sides of formed crack occurred and it maybe cause the formation of cracks in the weld. The formation of hot crack may be related with the formation of γ' phase at Ti and Al supersaturated places, but it needs another investigation to be confirmed.

**Fig. 10.** Variation of weld hardness versus welding heat input in Udimet 520.

3.2. Rockwell hardness profile of Udimet 520 weld

Fig. 10 shows the variation of hardness with input heat. Hardness of 42 HRC and 37 HRC achieved at input heat of 4300 J/mm and 6500 J/mm, respectively. It indicates that reducing the input heat of 2200 J/mm increased the hardness about 5 HRC. This reveals that the weld hardness depends on the weld input heat. The reasons of increment of the hardness are: (1) With decreasing input heat of the weld, critical rate of cooling increases and leads to the formation of columnar grains. Formation of columnar grains is one of the strengthening mechanisms in solidified metals. Also, because of high cooling rate, homogeneity of γ phase increases. (2) With decreasing of the input heat, tendency to the hot cracking and strain aging cracking decreases. Fig. 11 shows the change of hardness with increasing welding rate. Change of welding rate of about 0.5 mm/s increased the hardness to about 5 HRC. The strengthening factors due to increasing of welding rate are the same as what are explained for the effects of decreasing of welding heat. Crystal growth rate increases by enhancing welding rate as ($R = S \cos(\theta)$) where R is crystal growth rate, S is welding rate, and θ is angle between growth direction of crystal and welding direction. Therefore, tendency to columnar growth increases the hardness [2].

It was ascertained that physical and mechanical properties of metals change by dissolving any element in their lattice. This change is resulted from dereference between physical and crystallographic properties of solutes and parent phase such as lattice parameter and elasticity modulus [15]. Increment of yield strength depends upon the atomic size difference, position of solutes in periodic table relative to parent phase (number of empty electrons at valance layer), elastic modulus, the stacking fault energy, short range order and concentration of solutes [15–17]. W, Mo, Cr and Al are the main solid solution strengthening elements in Udimet 520. Although Co has significant effect on solid solution strengthening, it decreases the stacking fault energy because of large difference in lattice parameters. This makes the cross slip difficult, whereby the strength of metal increases [16,17]. Effect of solid solution strengthening is preserved up to 0.6 Tm (815 °C) while the strength of γ depends on atomic diffusion at temperature higher than 0.6 Tm. Consequently, the effect of Cr and Ti will be limited,

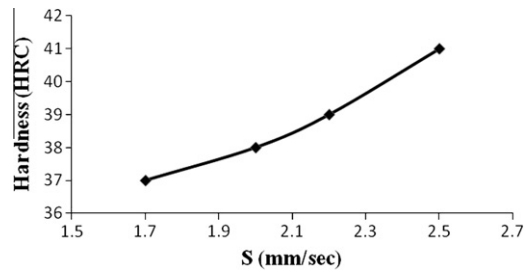


Fig. 11. Variation of welding speed versus weld hardness in Udimet 520.

and Mo and W will have important effect as restricting diffusion elements [14,15]. Reasons of increasing of the strength by addition of solutes are as follow [16,18]: generation of internal elastic strain field due to mismatch of lattice parameter and elastic modulus, decreasing of stacking fault energy and production of short range order. Dissolutions not only increase yield and tensile strengths but also they increase creep strength and endurance limit (fatigue strength) [18,19]. According to the strengthening mechanisms are discussed in the previous sections, improvement in hardness of the weld due to increasing welding rate and decreasing heat input is related with the fineness of columnar structure and solid solution strengthening.

4. Conclusions

In this paper, the Udimet 520 weld with cellular–dendritic and rarely dendritic structure including γ matrix rich of Cr, Mo and W as solid solution strengthening agents, low percentage associated with order morphology and relative uniform distribution of MC carbides was produced by GTAW. It was seen that Udimet 520 alloy has high resistance against hot cracking during welding. Hot cracking occurred only at high input heat values. Distribution of different element at sides of formed hot crack during welding at high input heat showed that cracking occurs at the places that the concentration of Al and Ti is high. Therefore, cracking may be related with the Ni₃Al (Ti) phase precipitation.

Also, Increasing of welding speed and decreasing input heat improved the hardness of the weld. Increase in hardness of GTA welded Udimet 520 due to increasing welding rate and decreasing

heat input is attributed to the fineness of columnar structure and solid solution strengthening.

References

- [1] Voort GFV. Metals handbook: wrought heat resistant alloys. Metals Park, Ohio: ASM International; 1996.
- [2] Porter DA, Easterling KE. Phase transformation in metals and alloys. London: Chapman and Hall; 1992. 318–321.
- [3] Idowu OA, Ojo OA, Chaturvedi MC. Effect of heat input on heat affected zone cracking in laser welded ATI Allvac 718 Plus superalloy. Materials Science & Engineering, A: Structural Materials: Properties, Microstructure and Processing 2007;454–455:389–97.
- [4] Ojo OA, Richards NL, Chaturvedi MC. Contribution of constitutional liquation of gamma prime precipitate to weld HAZ cracking of cast Inconel 738 superalloy. Scripta Materialia 2004;50:641–6.
- [5] Nematzadeh F, Akbarpour MR, Kokabi AH, Sadrnezhaad SK. Structural changes of radial forging die surface during service under thermo-mechanical fatigue. Materials Science & Engineering, A: Structural Materials: Properties, Microstructure and Processing 2009;527:98–102.
- [6] Xu S, Koul AK, Dickson JL. Creep crack growth in the absence of grain boundary precipitates in Udimet 520. Metallurgical and Materials Transactions A: Physical Metallurgy and Materials Science 2001;32:795.
- [7] Jahazi M, Mashreghi AR. Dissolution and precipitation kinetics of [gamma]' in nickel base superalloy. Mater Sci Tech 2002;18:458.
- [8] Xu S, Dickson JL, Koul AK. Grain growth and carbide precipitation in superalloy Udimet 520. Metallurgical and Materials Transactions A: Physical Metallurgy and Materials Science 1998;204.
- [9] Reed PAS, Wu XD, Sinclair I. Fatigue crack path prediction in udimet 720 Nickel – based alloy single crystals. Metallurgical and Materials Transactions A: Physical Metallurgy and Materials Science 2000;31:109–23.
- [10] Duvall DS, Owczarski WA. Further heat affected zone studies in heat resistant Nickel alloys. Welding J 1997;46:4235–325.
- [11] Oktay Alniak M, Bedir Fevzi. Hot forging behavior of nickel based superalloys under elevated temperatures. Mater Design 2010;31:1588–92.
- [12] Savage WF, Jackson CE. Microsegregation in autogeneous hast alloy x. Weld J 1971;50:302s–3s.
- [13] William O, Owczarski A. Process and metallurgical factors in jointing superalloy and other high service temperature materials. Phys Metall Metals Joint AIME 1980:369–409.
- [14] Lachowicz M, Dudzinska W, et al. Microstructure transformations and cracking in the matrix of γ – γ' superalloy Inconel 713C melted with electron beam. Materials Science & Engineering, A: Structural Materials: Properties, Microstructure and Processing 2008;479:269–76.
- [15] Cheng KY, Jo CY, Jin T, Hu ZQ. Influence of applied stress on the γ' directional coarsening in a single crystal superalloy. Mater Design 2010;31:968–71.
- [16] Gyekenyesi AL, Kautz HE, Shannon RE. Quantifying creep damage in a metallic alloy using acousto-ultrasonics. JMEPEG 2002;11:205–10.
- [17] Mashreghi AR, Monajatizadeh H, Jahazi M, Yue S. High temperature deformation of nickel base superalloy Udimet 520. Mater Sci Tech 2004;20:161.
- [18] Chiozzi S, Dattoma V, Panella F. Capacitor discharge welded bars of Inconel 718 and TiAl6V4 superalloys under fatigue. Mater Design 2008;29:839–51.
- [19] Rahmani Kh, Nategh S. Isothermal LCF behavior in aluminide diffusion coated René 80 near the DBTT. Mater Design 2009;30:1183–92.